RSC Advances

This is an *Accepted Manuscript*, which has been through the Royal Society of Chemistry peer review process and has been accepted for publication.

Accepted Manuscripts are published online shortly after acceptance, before technical editing, formatting and proof reading. Using this free service, authors can make their results available to the community, in citable form, before we publish the edited article. This *Accepted Manuscript* will be replaced by the edited, formatted and paginated article as soon as this is available.

You can find more information about *Accepted Manuscripts* in the Information for Authors.

Please note that technical editing may introduce minor changes to the text and/or graphics, which may alter content. The journal's standard Terms & Conditions and the Ethical guidelines still apply. In no event shall the Royal Society of Chemistry be held responsible for any errors or omissions in this *Accepted Manuscript* or any consequences arising from the use of any information it contains.

ROYAL SOCIETY OF CHEMISTRY

www.rsc.org/advances

RSC Advances

RSCPublishing

PAPER

Energy transfer from Bi^{3+} to Ho^{3+} triggers brilliant single green light emitting in $LaNbTiO_6$: Ho^{3+}, Bi^{3+} phosphors

Cite this: DOI: 10.1039/xoxxoooooox

Xingshuang Zhang[a], Guangjun Zhou[a,*], Juan Zhou[b], Haifeng Zhou[a], Peng Kong[a], Zhichao Yu[a], Jie Zhan[a]

Received ooth January 2012,
Accepted ooth January 2012

DOI: 10.1039/xoxxoooooox

www.rsc.org/

Excitation of Ho^{3+} and Bi^{3+} co-doped $LaNbTiO_6$ particles with 453 nm blue light gave an intense single green glow. All the phosphors were synthesized via a facile sol-gel and combustion approach, and the crystal structure, particle morphology, photoluminescence (PL) properties of the phosphors and energy transfer between Bi^{3+} and Ho^{3+} were also investigated. The largely spectral overlap between the broad emission band of Bi^{3+} around 425~570 nm and the excitation band of Ho^{3+} supports the efficient energy transfer from Bi^{3+} to Ho^{3+}, which enhance the PL intensity remarkably. When the PL intensity is considered, the best composition for producing green light is $LaNbTiO_6$: 4 mol% Ho^{3+}, 2 mol% Bi^{3+}. The luminous mechanisms of Ho^{3+} doped and Ho^{3+}/Bi^{3+} co-doped in the $LaNbTiO_6$ host were also discussed.

Introduction

Over the past several decades, activation of rare earth (RE) compounds by various lanthanide ions has been extensively investigated owing to the fascinating optical characteristics based on their unique intra-4f transitions that could result in long-lived luminescent excited states and narrow emission bands. At the same time, lanthanide ions involved intra-4f transitions are barely affected by external environment or crystal field on account of the shielding of the 4f orbits by the filled outer 5s and 5p orbits.[1-3] In view of the above mentioned facts, some luminescent materials have been widely applied in lighting, display fields and biological applications.[4-7] As we all know, the production of white light by means of combination of red, green, and blue phosphors with a near-ultraviolet or ultraviolet diode is highly favoured. In view of the huge potential market in home lighting, many LED manufacturers globally want to develop them. Therefore, faced with this trend, new-type highly efficient red, green, and blue phosphors must be developed rapidly so as to keep up with the advances made in diode emission wavelength.[8,9]

Ho^{3+} possesses a wealth of energy levels and, consequently, has many luminescent states due to the complexity of the $4f^{10}$ energy level system.[10] Malinowski et al. pointed out that Ho^{3+} systems have been investigated for application in infrared lasers for remote sensing and medical purposes.[11] Extensive investigations of the optical spectra of Ho^{3+} have been carried out for $M_3Al_5O_{12}$: Ho^{3+} (M=Y, Lu),[12] $MLiF_4$: Ho^{3+} (M=Gd, Y, Lu),[13] $MBi(XO_4)$: Ho^{3+} (M=Li, Na; X=W, Mo).[14] In addition, researchers have reported that Bi^{3+} usually acts as an excellent sensitizer for RE ions in a variety of hosts such as rare earth oxides, phosphates, molybdates, vanadates, tungstates and nibobates, for instance, Y_2O_3: Bi^{3+}, Ln^{3+} (Ln=Sm, Eu, Dy, Er, Ho),[15] YPO_4: Bi^{3+}, Eu^{3+},[16] $CaMoO_4$: Bi^{3+}, Eu^{3+},[17] MVO_4: Bi^{3+}, Ln^{3+} (M=Y, Gd; Ln=Eu, Sm, Dy, Ho, Yb),[18-22] $ZnWO_4$: Eu^{3+}, Bi^{3+},[23, 24] $LnNbO_4$: Dy^{3+}, Bi^{3+} (Ln=La, Y, Gd).[25] All these stem from the fact that the UV efficiency of the phosphors can be remarkably enhanced by the energy transfer (ET) from Bi^{3+} to RE ions under the excitation of UV light. Compared with other rare earth elements, La is more abundant in rare earth mineral resources and lanthanum oxide is much cheaper than other rare earth oxides. Nevertheless, the development of La-based materials is still inadequate and lanthanum oxide is overstocked in the rare earth industry. Therefore, it is fairly valuable to fundamentally and practically study the La-based materials for the balanced-utilization of the rare earth natural resources.[26] Although many lanthanum compounds materials with various morphologies such as nanospheres, nanorods, nanowires, and nanoplates etc. have been synthesized in the past few years, lanthanum titanoniobates doped with RE ions as well as their optical properties have rarely been investigated up to now. In addition, for conventional powder phosphors, reduction in the particle size is achieved by mechanically grinding techniques. While this mechanically grinding method easily results in formation of large amount of surface defects which provides non-radiative recombination process, and ultimately decreases the luminescent efficiency.[27] Therefore, the direct preparation of luminescent materials in nanoscale has become vital.

Herein, a facile combinatorial chemistry approach, characterized by sol-gel and combustion was employed to synthesize the Ho^{3+}, Bi^{3+} co-doped $LaNbTiO_6$ powder phosphors with aeschynite-type structure. During the course of spectroscopic investigations on Ho^{3+} and Bi^{3+} co-doped $LaNbTiO_6$, strong green emitting originate from Ho^{3+} and Bi^{3+} was observed under 453 nm excitation. Besides, the mechanism of the energy transfer from Ho^{3+} to Bi^{3+} was also discussed.

RSC Advances Accepted Manuscript

Experimental

Synthetic procedures

Pure and doped $LaNbTiO_6$ samples were synthesized via a facile sol-gel and combustion process. Lanthanum oxide, holmium oxide, bismuth nitrate, niobium oxide, tetra-n-butyl titanate, nitric acid, hydrofluoric acid (HF, 40 %), ammonium nitrate, citric acid were used as starting materials to prepare the phosphor samples. All the reagents were used without further purification. Lanthanum nitrate and holmium nitrate solutions were produced previously by dissolving the lanthanum oxide and holmium oxide with excess diluted nitric acid, respectively. The acquired lanthanum nitrate and holmium nitrate solutions were heated at 120 ^oC to evaporate distilled water and the excess nitric acid. Then, the lanthanum nitrate and holmium nitrate solid were made up to solutions of 0.5 $mol{\cdot}L^{-1}$ and 0.05 $mol{\cdot}L^{-1}$, respectively. Citric acid was not only used as prominent complexant for sol process in aqueous solution, but also facilitated the formation of gel. Meanwhile, citric acid and ammonium nitrate with the mole ratio of 1:5 acted as fuels for the combustion process.

Firstly, 0.5 mmol Nb_2O_5 was dissolved with excess hydrofluoric acid in a water bath at 90 ^oC, and the pH of the NbF_5 solution was regulated to 9.0 by adding ammonia aqueous solution. Then, the white precipitate of niobic acid obtained was filtered and washed with deionized water for several times to make sure that the F^- ions were completely removed. Afterward, the precipitate of niobic acid was dissolved with tetra-n-butyl titanate and citric acid with the mole ratio of 1:1:3 under heating at 80 ^oC. Then, tetra-n-butyl titanate, lanthanum nitrate, and ammonium nitrate with the mole ratio of 1:1:15 were added and mixed homogeneously under continuous stirring and heating at 80 ^oC for 4~5 h until the sol formed. After the water evaporated, the transparent sol turned into gel with high viscosity. The gel was dried at 120 ^oC for 16 h to form yellow xerogel. The obtained xerogel was then introduced into crucibles, then directly transferred into a muffle furnace annealed at 1100 ^oC for 1 h, respectively. Finally, all samples were ground into powder for characterization. The synthesis processes of Ho^{3+}-doped, Bi^{3+}-doped and Ho^{3+}, Bi^{3+} co-doped $LaNbTiO_6$ could refer to SI.

Characterization

The phase composition and structure were characterized using X-ray powder diffraction patterns (Germany Bruker Axs D8-Avance X-ray diffractometer with graphite monochromatized Cu Kα irradiation (λ = 1.5418 Å)), and all the data were collected with the 2θ range of 10-80^o, step width of 0.02^o and count time of 0.2 s/step. Thermal analysis of the powder that was dried at 120 ^oC for 16 h was carried out from 30 to 1000 ^oC by thermogravimetry-differential thermal analysis (TG-DTA) (PerkinElmer Corporation, Diamond TG-DTA) with a constant heating rate of 20 ^oC/min. The microstructure and stoichiometry data were obtained by SEM (Hitachi, S-4800) and EDS (Horiba EMAX Energy, EX-350), respectively. The PL property measurements were recorded on a fluorescence spectrophotometer (JEOL, F-4500 and FLS920), and a 450 W Xe lamp serves as the excitation source. The absolute quantum efficiencies of the phosphor were measured on an Edinburgh FLS920 fluorescence spectrometer and its quantum yield measurement system. In addition, a fluorescence microscope (Nikon Eclipse 80i) was used for the luminescence observation of the samples. All the measurements were taken at room temperature.

Results and discussion

Structure and morphology

It is well known that the crystallinity, crystallite size and surface morphology have a strong influence on the PL properties of phosphor materials. Our previous work have verified that the best crystallinity of pure $LaNbTiO_6$ crystals can be successfully synthesized via a facile method after being annealed at 1100 ^oC for 1h, and the PL intensity of doped phosphors is optimal at the same time. Consequently, all the samples were annealed at 1100 ^oC for 1h ultimately in this study.

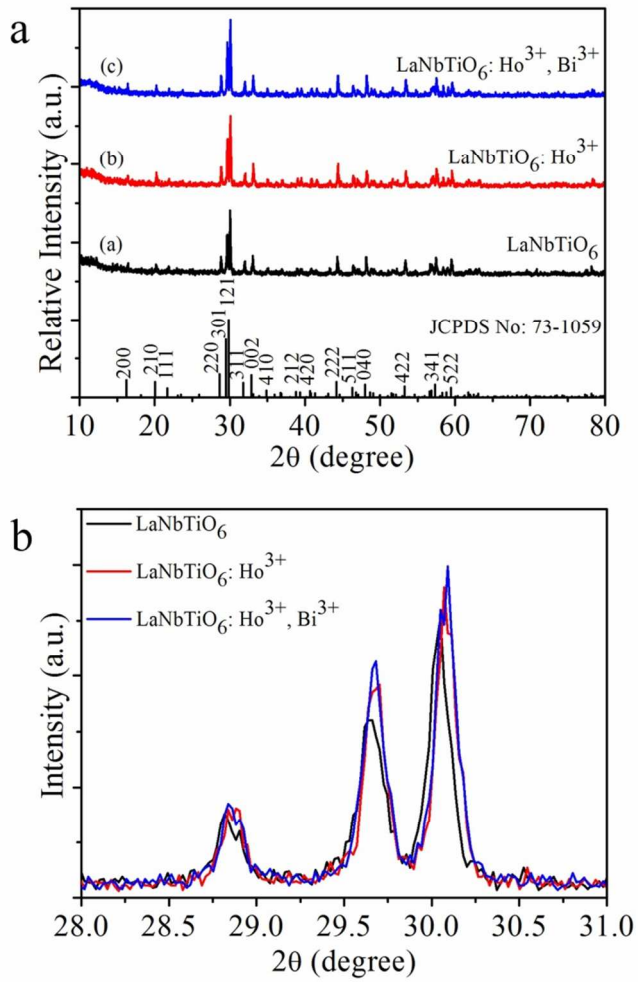

Fig. 1 (a) XRD patterns of the as-synthesized pure $LaNbTiO_6$, $LaNbTiO_6$: 4 mol% Ho^{3+} and $LaNbTiO_6$: 4 mol% Ho^{3+}, 2 mol% Bi^{3+} samples annealed at 1100 ^oC for 1 h successively as well as the JCPDS card 73-1059 of $LaNbTiO_6$ for comparison. (b) Comparison of the samples as-synthesized from 2 θ of 28.0 degree to 31.0 degree.

The composition and phase purity of the as-prepared pure and doped $LaNbTiO_6$ products were first measured by XRD. Fig. 1 (a) shows the XRD patterns of pure $LaNbTiO_6$, $LaNbTiO_6$: 4 mol% Ho^{3+} and $LaNbTiO_6$: 4 mol% Ho^{3+}, 2 mol%

RSC Advances Accepted Manuscript

This journal is © The Royal Society of Chemistry 2014

Bi^{3+} phosphors, and all the diffraction peaks of the as-synthesized sample are in good agreement with aeschynite-type $LaNbTiO_6$ (Joint Committee on Powder Diffraction Standards JCPDS File Card No. 73-1059). This can be explained that rare earth ions have similar co-ordination structure and atomic radius, as a result the crystal structure does not change dramatically when the metal ions (La^{3+}) are replaced by one or more kinds of RE ions. The main peaks (200), (210), (111), (220), (301), (121), (311), (002) and so on are well indexed in the standard pattern, respectively. From the XRD patterns, it was confirmed that no separate Ho^{3+} or Bi^{3+} related phases were detected at the current doped level, indicating that the pure $LaNbTiO_6$ crystals were successfully prepared via this facile method. Furthermore, according to JCPDS No. 73-1059 data file, $LaNbTiO_6$ crystallizes as a orthorhombic structure with a space group of Pnma (62), and lattice parameters were achieved with a= 10.934 Å, b= 7.572 Å, c= 5.446 Å, with volume unit cell of 450.9 $Å^3$ and Z= 4. At the same time, the trivalent Ho^{3+} and Bi^{3+} ions have been effectively incorporated into the $LaNbTiO_6$ host by substituting La^{3+} because of their similar ionic radius. The ionic radii for eight-coordinated La^{3+}, Ho^{3+}, and Bi^{3+} are 1.172 Å, 1.041 Å, and 1.170 Å, respectively. In addition, it can be observed from Fig. 1 (b) that the diffraction peaks positions are slightly shifted to a greater degree when Ho^{3+} or Ho^{3+}/Bi^{3+} ions were doped into the $LaNbTiO_6$ host, which can be attributed to the decrease of the interplanar spacing owing to the substitution of larger-size La^{3+} sites by the smaller-size Ho^{3+} and Bi^{3+}, leading to the lattice distortion effect, and decrease of lattice parameters and volume accordingly. The XRD results demonstrating that the structure of $LaNbTiO_6$ host lattice and phase composition of phosphors in our experimental range were unchanged upon the doping of Ho^{3+} ions or the co-doping of Ho^{3+}/Bi^{3+}.

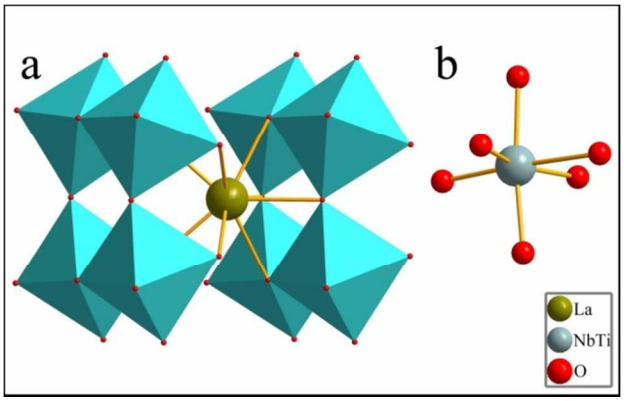

Fig. 2 (a) Three-dimensional space crystal structure of $LaNbTiO_6$, and (b) balls-sticks model of NbTi-O octahedron.

According to the lattice parameters and the related files provided by American Mineralogist Crystal Structure Database, the three-dimensional structure diagram was described in Fig. 2. From the crystal structure of $LaNbTiO_6$ in Fig. 2 (a), the blue octahedrons represent the NbTi-O groups, in the meantime, La^{3+} is in the center of the eight NbTi-O octahedrons, and Ho^{3+}/Bi^{3+} will substitute La^{3+} to occupy this position in the Ho^{3+} doped or Ho^{3+}/Bi^{3+} co-doped phosphors. In addition, from the balls-sticks model of NbTi-O groups in Fig. 2 (b), it can be found that NbTi is in the center of the octahedron which is composed of six oxygen atoms.

Fig. 3 shows the TG-DTA curves of pure $LaNbTiO_6$ precursor xerogel powder that is the yellow xerogel dried at 120 °C for 16 h. The TG curve displays three main weight loss stages. At the first stage, weight loss is about 69.32 % below 288 °C. Moreover, in the DTA curve, there are two weak exothermic peaks around 127 and 197 °C owing to cross-link effect, and one exothermic peak at 246 °C on account of combustion of organic components such as citric acid or the remaining organic components from tetra-n-butyl titanate and decomposition of the complex compound. The second stage of weight loss is approximately 8.26 %, mainly because of the further combustion of the citrate and the organic residues, such as the oxidation and dehydroxylation of the decomposers, accompanied by one sharp exothermic peak in the DTA curve from 288 to 596 °C at the same time. Weight loss of the third stage is about 8.06 %, accompanied by one obviously exothermic peak at 764 °C which can be ascribed to the process of monoclinic and orthorhombic phase formation, crystallization and transition.[28] Once the combustion process reached an end, the sample underwent no further transformations and there is nearly no weight loss in the TG curve when the temperature is above 950 °C, which illustrates that the sample has reached a relatively stable state in the process of phase transition.

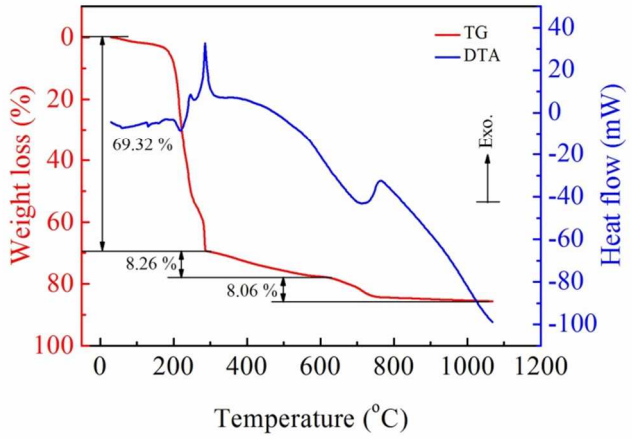

Fig. 3 TG-DTA curves of pure $LaNbTiO_6$ precursor xerogel powder.

Fig. 4 shows typical scanning electron microscope (SEM) images of pure and doped samples at 1100 °C for 1h. The sample exhibits agglomeration phenomenon due to sintering at high temperature, resulting in irregular particle shapes. By taking agglomeration effects into account, many particles of $LaNbTiO_6$ in Fig. 4a formed plates or blocks whose diameters are up to 400~800 nm. From the micrograph of $LaNbTiO_6$: 4 mol% Ho^{3+} in Fig. 4b, it can be seen that morphology of the as-synthesized samples is similar to that in Fig. 4a and there are short rods and some irregular particles form from several adjacent particles connect and agglomerate with each other. Similarly, Fig. 4c demonstrates the image of $LaNbTiO_6$: 4 mol% Ho^{3+}, 2 mol% Bi^{3+}. These particles become smaller than that of pure $LaNbTiO_6$ and $LaNbTiO_6$: 4 mol% Ho^{3+} overall, almost below 500 nm. That is to say, the agglomeration effect could be weakened when doped with Ho^{3+} or Ho^{3+}/Bi^{3+} co-doped in the host. Further evidence concerning composition of the 4 mol%

RSC Advances Accepted Manuscript

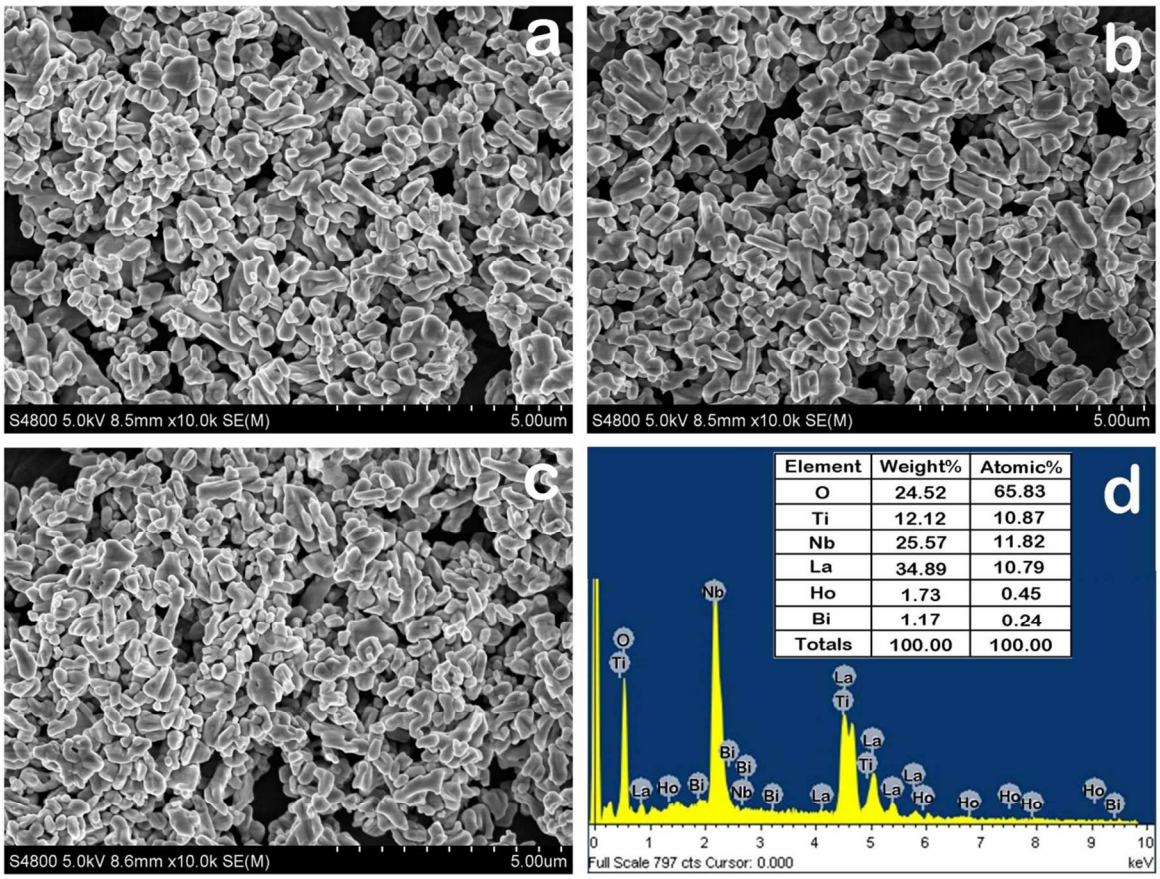

Fig. 4 SEM micrographs of pure and doped samples obtained at 1100°C for 1h: (a) $LaNbTiO_6$; (b) $LaNbTiO_6$: 4 mol% Ho^{3+}; (c) $LaNbTiO_6$: 4 mol% Ho^{3+}, 2 mol% Bi^{3+}; and (d) EDS spectrum of $LaNbTiO_6$: 4 mol% Ho^{3+}, 2 mol% Bi^{3+} sample and the inset shows the weight percent and atom percent of all elements.

Ho^{3+} and 2 mol% Bi^{3+} co-doped $LaNbTiO_6$ sample was achieved by energy dispersive X-ray spectrometer (EDS) spectrum which is presented in Fig. 4d. By means of multiple tests and calculating on the subject of EDS spectra, the ratio of M(La, Ho, Bi)/Nb/Ti/O is 1.06:1.09:1:6.06, very close to M/Nb/Ti/O=1:1:1:6, indicating that the sample probably is composed of $LaNbTiO_6$. Furthermore, the ratio of Ho/M is 3.92 % by calculating in the EDS spectra, close to 4 % as well, and the ratio of Bi/M is 2.09 %, which is close to 2 %, demonstrating that corresponding Ho^{3+} and Bi^{3+} ions were incorporated into the host successfully.

Photoluminescence properties

Fig. 5 shows the excitation spectra, emission spectra and energy level diagram of $LaNbTiO_6$: x mol% Ho^{3+}. Fig. 5 (a) displays the excitation spectra of the phosphors monitored with emission wavelength at 545 nm, and all the excited peaks could be ascribed to the typical Ho^{3+} intra-$4f^{10}$ transition absorption. According to the energy level diagram in the inset of Fig. 5 (a) and the labels over the excited peaks, it can be found that all the excited peaks originate from the ground state $^5I_8$ energy level of Ho^{3+} transfers to the higher excited state energy levels. For example, the sharpest excitation band around 453 nm is derived from the transition from the ground state $^5I_8$ energy level to $^5F_1$ and $^5G_6$. Similarly, excitation band at 521 nm ($^5I_8 \rightarrow {}^5F_4$) and five weak excitation bands located at 361 nm ($^5I_8 \rightarrow {}^3H_6$), 393 nm ($^5I_8 \rightarrow {}^5G_4$), 420 nm ($^5I_8 \rightarrow {}^5G_5$), 478 nm ($^5I_8 \rightarrow {}^5F_2$) and 490 nm ($^5I_8 \rightarrow {}^5F_3$), respectively.[29, 30] Therefore, it can be also found that blue laser diodes and light emitting diodes may be efficient pumping sources in obtaining Ho^{3+} emissions. Hereby, it can be inferred that the excitation light at 453 nm can make the electrons jump from excited state to ground state, and decline to lower energy level through non-radiative transitions and relaxation effect between multi-photons. Fig. 5 (b) presents the emission spectra of the $LaNbTiO_6$: x mol% Ho^{3+} (x=0.5~5) under excitation at 453 nm. All these energy transitions are also ascribed to the characteristic f-f transitions of Ho^{3+}. The green emission peak at 545 nm could be ascribed to the transition of Ho^{3+} from excited state $^5F_4$ and $^5S_2$ to ground state $^5I_8$. Similarly, the other two weak emission peaks at 483 nm and 650 nm derived from $^5F_2 \rightarrow {}^5I_8$ transition and $^5F_5 \rightarrow {}^5I_8$ transition of Ho^{3+}, respectively. These can be supported by the inset of Fig. 5 (a). In addition, from the emission intensities at 545 nm as a function of the Ho^{3+} doped concentrations demonstrated in Fig. 5 (b), it can be seen that when the Ho^{3+} doped concentration varies from 0.5 to 4 mol%, the PL intensity increased first, and beyond that gradually decreased. That is to say, when the Ho^{3+} doped concentration is up to 4 mol%, the PL intensity reaches to the maximum. To sum all, Ho^{3+} acts as an activator in the host and makes the phosphors present strong green light through its characteristic emissions.

RSC Advances Accepted Manuscript

This journal is © The Royal Society of Chemistry 2014

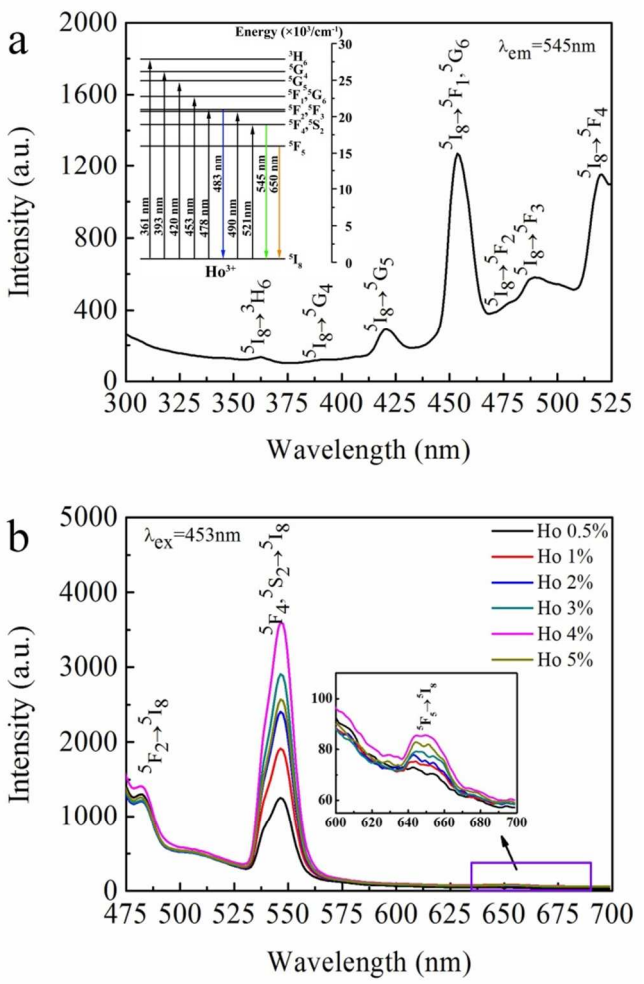

Fig. 5 (a) Excitation spectrum of Ho^{3+}-doped $LaNbTiO_6$ sample (λ_{em}=545 nm) and the inset is the energy level diagram of Ho^{3+} in $LaNbTiO_6$, (b) emission spectra of Ho^{3+}-doped $LaNbTiO_6$ samples prepared with a function of doped concentrations (λ_{ex}=453 nm).

Although Ho^{3+} possesses fairly rich energy structure ($4f^{10}$), and there are multiple characteristic emission line corresponding to $^5F_4+^5S_2\rightarrow{}^5I_8$ transitions (green light), $^5F_5\rightarrow{}^5I_8$ and $^5F_4+^5S_2\rightarrow{}^5I_7$ transitions (red light) could be measured.[31-33] While there is few reports concerning single green emission of Ho^{3+} doped phosphors materials so far. Under blue light LDs and LEDs pumping, $LaNbTiO_6$: Ho^{3+} phosphors could produce effective homogeneous green emission, and have potential application value in the field of flat panel display and trichromatic phosphor.

Doping a certain amount of sensitized ions into phosphors materials could affect the symmetry of the ligand field, and promote the process of the energy transfer which increases the PL intensity of the RE ions doped phosphors effectively. In addition, many reports confirmed that Bi^{3+} is a wonderful candidate in many hosts.[9, 16, 34] The electronic configuration of Bi^{3+} is $[Xe]4f^{14}5d^{10}6s^2$. The ground state is $^1S_0$ with $6s^2$ configuration and the excited states of the 6s6p configuration can be split into the $^3P_0$, $^3P_1$, $^3P_2$ and $^1P_1$ levels in an increasing energy order. The $^1S_0\rightarrow{}^3P_0$ transition is strongly spin forbidden, but the $^1S_0\rightarrow{}^3P_1$ and $^1S_0\rightarrow{}^3P_2$ transitions become allowed due to the spin-orbit coupling. For the $^1S_0\rightarrow{}^1P_1$ transition, it is an allowed electric dipole transition.[35] The $^3P_1$ level of Bi^{3+} is split into two and three sets of energy levels under S_6 and C_2 symmetry, respectively. The blue emissions is ascribed to the transition from the splitting $^3P_1$ levels to the ground state $^1S_0$ level of Bi^{3+} (S_6), and the green emission is assigned to the transition from the bottom of $^3P_1$ to $^1S_0$ level of Bi^{3+} (C_2).[36, 37] From the excitation spectrum and emission spectrum of $LaNbTiO_6$: Bi^{3+} in Fig. 6, it can be found that Bi^{3+} has a strong absorption around the 328 nm and the broad blue-green emission band around 425~570 nm largely overlaps with the excitation band of Ho^{3+}. Therefore, it could be inferred that the incorporation of Bi^{3+} could enhance the PL intensity of $LaNbTiO_6$: Ho^{3+}, in addition, $LaNbTiO_6$: Ho^{3+}, Bi^{3+} phosphors were prepared and the PL properties were also studied in the next experiment.

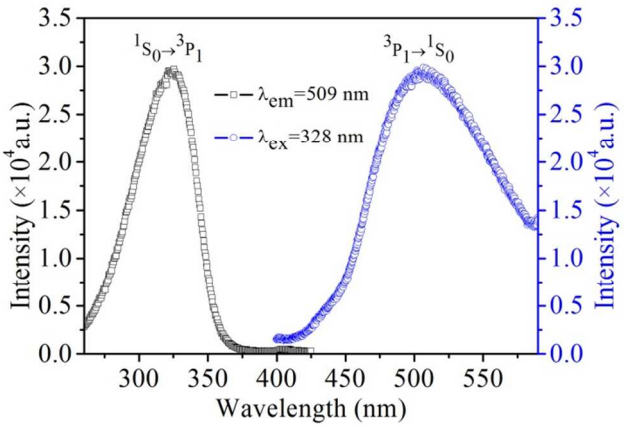

Fig. 6 Excitation spectrum (λ_{em}=509 nm) and emission spectrum (λ_{ex}=328 nm) of $LaNbTiO_6$: Bi^{3+} sample.

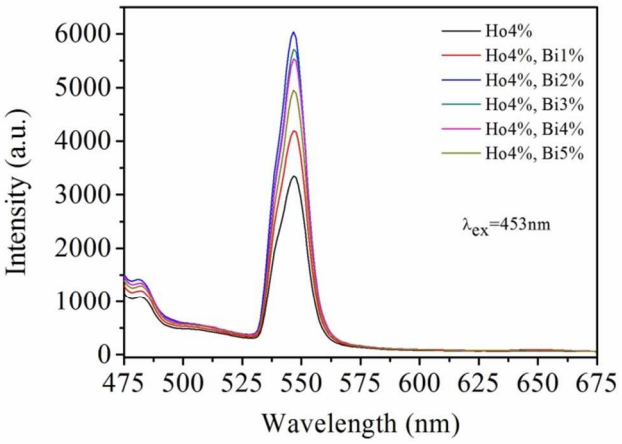

Fig. 7 Emission spectra of Ho^{3+}, Bi^{3+} co-doped $LaNbTiO_6$ samples prepared with a function of concentrations of Bi^{3+} under excitation at 453 nm.

Fig. 7 presents the emission spectra (λ_{ex}= 453 nm) of $LaNbTiO_6$: 4 mol% Ho^{3+}, y mol% Bi^{3+} (y=0~5) as a function of the Bi^{3+} doped concentrations under excitation at 453 nm. Comparison with $LaNbTiO_6$: 4 mol% Ho^{3+}, the strongest emission peak position still located at 545 nm when Bi^{3+} was doped in the host, while the PL intensity at 545 nm increases dramatically that could be up to 1.8 times of $LaNbTiO_6$: 4 mol% Ho^{3+}. Generally speaking, there are two kinds of energy transfer

RSC Advances Accepted Manuscript

mechanism as to the phenomenon of sensitization. One is radiation energy transfer that the luminescence of sensitizer was absorbed by the activator, and the other is non-radiation energy transfer produced by the multipole interaction between sensitizer and activator, which is electric dipole and electric dipole interaction, electric dipole and electric quadrupole interaction, or electric quadrupole and electric quadrupole interaction. While in the system of $LaNbTiO_6$: 4 mol% Ho^{3+}, 2 mol% Bi^{3+}, the characteristic peaks of Ho^{3+} do not change, while no characteristic peak of Bi^{3+} is detected, indicating that efficient energy levels from Bi^{3+} to Ho^{3+} occurs. Under the excitation at 453 nm, the host absorbs energy, and the charge transfer occurs from $NbTiO_6^{3-}$ to Bi^{3+} and Ho^{3+}. Moreover, $^3P_1$ excited state of Bi^{3+} could transfer energy to Ho^{3+}, promoting the energy transition of Ho^{3+} and enhancing the PL intensity. The effective energy transfer process $Bi^{3+}\rightarrow Ho^{3+}$ is mainly through the radiation energy transfer of Bi^{3+} to increase the f-f transitions of Ho^{3+}. Accordingly, when Bi^{3+} was introduced into the host, Bi^{3+} can efficiently transfer its absorption energy to Ho^{3+}.

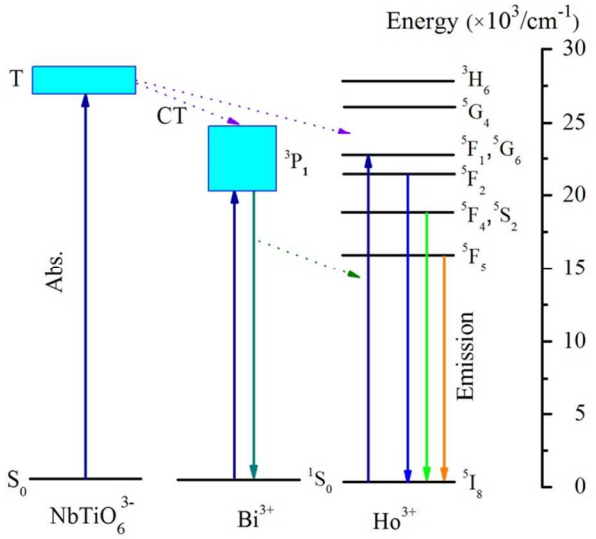

Fig. 8 Schematic diagram of $NbTiO_6^{3-}$, Bi^{3+}, and Ho^{3+} energy levels, excitation, emission, and energy transfer in $LaNbTiO_6$.

Accordingly, the excitation and emission processes of $LaNbTiO_6$: Ho^{3+}, Bi^{3+} luminescence can be summarized in Fig. 8. Apart from that, in the host of $LaNbTiO_6$, it is easy for Bi^{3+} to substitute La^{3+} (1.172 Å) and occupy the lattice sites with a low symmetry for the radius of Bi^{3+} (1.170 Å) is slightly smaller than that of RE^{3+}. The doping of Bi^{3+} could increase the disorganization of the ambient environment around Ho^{3+} which is also advantageous to improve the PL intensity of Ho^{3+}. From the emission spectra of Fig. 7, it can be found that the optimum doped concentration of Bi^{3+} is 2 mol%. Because of the radiation energy transfer of $Bi^{3+}\rightarrow Ho^{3+}$, the emission intensity of the phosphors increases with the doped concentration of Bi^{3+} within certain limits. However, once the doped concentration of Bi^{3+} exceeds 2 mol%, non-radiation energy transfer of $Bi^{3+}\rightarrow Bi^{3+}$ increases remarkably and energy transfer of $Bi^{3+}\rightarrow Ho^{3+}$ is weakened, resulting in the decrease of PL intensity, which is generally called concentration quenching.

The chromaticity coordination of $LaNbTiO_6$: 4 mol% Ho^{3+} and $LaNbTiO_6$: 4 mol% Ho^{3+}, 2 mol% Bi^{3+} is converted to the x, y CIE (Commission Internationale deI' Eclairage) 1931 chromaticity diagram in Fig. 9 The CIE chromaticity coordinates of the $LaNbTiO_6$: 4 mol% Ho^{3+} and $LaNbTiO_6$: 4 mol% Ho^{3+}, 2 mol% Bi^{3+} phosphors are (0.244, 0.550) and (0.256, 0.587), respectively, both corresponding to green emission in a different proportion. The absolute quantum efficiencies of the phosphors are 9 % ($LaNbTiO_6$: 4 mol% Ho^{3+}) and 16 % ($LaNbTiO_6$: 4 mol% Ho^{3+}, 2 mol% Bi^{3+}). Furthermore, the microscope fluorescence images of the Ho^{3+} doped, Ho^{3+} and Bi^{3+} co-doped $LaNbTiO_6$ are presented in the inset of Fig. 9, and both the two kinds of phosphors are under blue light excitation being magnified 40 times. It is clear that the images present a green color with high brightness and high homogeneity.

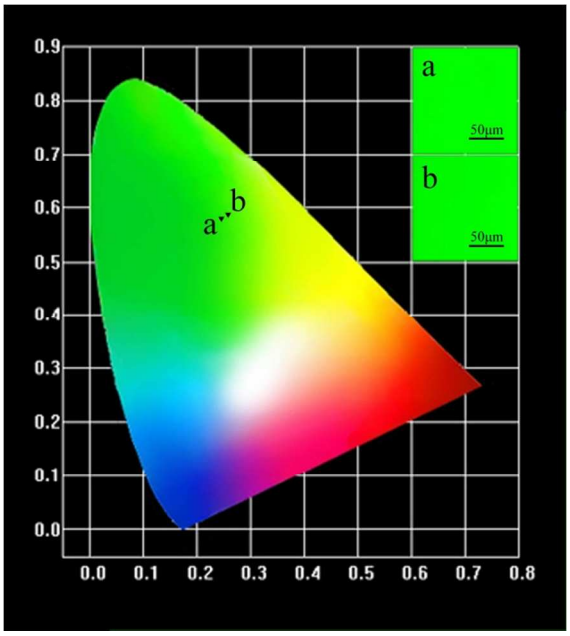

Fig. 9 CIE chromaticity diagram and microscope fluorescence images for (a) $LaNbTiO_6$: 4 mol% Ho^{3+} and (b) $LaNbTiO_6$: 4 mol% Ho^{3+}, 2 mol% Bi^{3+} phosphors.

Conclusions

A single green light emitting phosphor $LaNbTiO_6$: Ho^{3+}, Bi^{3+} was synthesized via a sol-gel and combustion approach. It has been found that Ho^{3+} and Bi^{3+} were incorporated into the $LaNbTiO_6$ though studying the crystal structure, and particle morphology. Moreover, the photoluminescence properties of Ho^{3+}-doped and Ho^{3+}, Bi^{3+} co-doped $LaNbTiO_6$ green phosphors also were investigated. With the activating of Ho^{3+}, under excitation at 453 nm blue light, emission spectra of the phosphors $LaNbTiO_6$: Ho^{3+} exhibited the strongest green light glow at about 545 nm owing to $^5F_4+^5S_2\rightarrow{}^5I_8$ transition of Ho^{3+} ions. In addition, it has been found that the broad emission band originating from $^3P_1\rightarrow{}^1S_0$ transition of Bi^{3+} overlaps with excitation band of Ho^{3+} though researching the excitation spectrum and emission spectrum of Bi^{3+}. Therefore, when Bi^{3+} and Ho^{3+} were co-doped into $LaNbTiO_6$, Bi^{3+} acts as an effective sensitizer of Ho^{3+}, inducing the energy transfer of $Bi^{3+}\rightarrow Ho^{3+}$and increasing the PL intensity remarkably. Considering the PL intensity, the best composition for

RSC Advances Accepted Manuscript

This journal is © The Royal Society of Chemistry 2014

producing green light is $LaNbTiO_6$: 4 mol% Ho^{3+}, 2 mol% Bi^{3+}, and the PL intensity of $LaNbTiO_6$: 4 mol% Ho^{3+}, 2 mol% Bi^{3+} was enhanced by 1.8 times than that of $LaNbTiO_6$: 4 mol% Ho^{3+} at 545 nm. Finally, the microscope fluorescence images and CIE chromaticity picture visually exhibit the emitting colors of Ho^{3+} doped and Ho^{3+}/Bi^{3+} co-doped in phosphors. From the above, preliminary studies have indicated that the $LaNbTiO_6$: Ho^{3+}, Bi^{3+} may have potential application value in the field of flat panel display and trichromatic phosphor, serving as a wonderful green light phosphor under blue light excitation.

Acknowledgements

This work was supported by projects from The Chinese PLA Medical Science and Technique Foundation (CWS11J243); Independent Innovation Foundation of Shandong University, IIFSDU (2011JC024); National Science Foundation of China (51372138) and The Scientific Research Foundation for the Returned Overseas Chinese Scholars, State Education Ministry.

Notes and references

[a] State Key Laboratory of Crystal Materials, Shandong University, Jinan 250100, P. R. China.
[b] Center for Disease Prevention and Control of Jinan Military Command, Jinan 250014, P. R. China.
* Corresponding author. Fax: +86 531 88361206
E-mail address: gjzhou@sdu.edu.cn

1. Y. Ding, S. Yu, C. Liu and Z. Zang, *Chem. Eur. J.*, 2007, **13**, 746.
2. C. Zhong, P. Yang, X. Li, C. Li, D. Wang, S. Gai and J. Lin, *RSC Adv.*, 2012, **2**, 3194.
3. G. Zatryb, A. Podhorodecki, J. Serafińczuk, M. Motyka, M. Banski, J. Misiewicz, N.V. Gaponenko, *Opt. Mater.*, 2013, **35**, 2090.
4. L. Li, W. Zi, G. Li, S. Lan, G. Ji, S. Gan, H., X. Xu, *J. Solid State Chem.*, 2012, **191**, 175.
5. U. Rambabu, S. Han, *RSC Adv.*, 2013, **3**, 1368.
6. G. Wang, Q. Peng and Y. Li, *Acc. Chem. Res.*, 2011, **44**, 322.
7. E. Téllez-Flores, R. Aceves, R. Pérez-Salas, I. Camarillo, U. Caldiño, *J. Lumin.*, 2013, **144**, 22.
8. L. Chen, K. Chen, C. Lin, C. Chu, S. Hu, M. Lee and R. Liu, *J. Comb. Chem.*, 2010, **12**, 587.
9. İ. Şabikoğlu, *J. Alloys Compd.*, 2013, **556**, 135.
10. P. A. Tanner, M. D. Faucher, and X. Zhou, *J. Phys. Chem. A*, 2011, **115**, 2557.
11. M. Malinowski, M. Kaczkan, A. Wnuk and M. Szuflinska, *J. Lumin.*, 2004, **106**, 269.
12. B. M. Walsh, G. W. Grew and N. P. Barnes, *J. Phys. Chem. Solids*, 2006, **67**, 1567.
13. B. M. Walsh, G. W. Grew and N. P. Barnes, *J. Phys.: Condens. Matter*, 2005, **17**, 7643.
14. A. Méndez-Blas, M. Rico; V. Volkov, C. Zaldo and C. Cascales, *Phys. Rev. B*, 2007, **75**, 174208.
15. G. Ju, Y. Hu, L. Chen, X. Wang, Z. Mu, H. Wu and F. Kang, *J. Lumin.*, 2012, **132**, 1853.
16. M. Niraj Luwang, R. S. Ningthoujam, S. K. Srivastava and R. K. Vatsa, *J. Am. Chem. Soc.*, 2011, **133**, 2998.
17. S. Yan, J. Zhang, X. Zhang, S. Lu, X. Ren, Z. Nie and X. Wang, *J. Phys. Chem. C*, 2007, **111**, 13256.
18. Y. Chen, Y. Wu, D. Wang and T. Chen, *J. Mater. Chem.*, 2012, **22**, 7961.
19. D. Chen, Y. Yu, P. Huang, Hang Lin, Z. Shan, L. Zeng, A. Yang and Y. Wang, *Phys. Chem. Chem. Phys.*, 2010, **12**, 7775.
20. U. Rambabu and S. Han, *Ceram, Int.*, 2013, **39**, 1603.
21. U. Rambabu, N. R. Munirathnam, S. Chatterjee, B. Sudhakar Reddy and S. Han, *Ceram, Int.*, 2013, **39**, 4801.
22. C. V. Devi, G. Phaomei, N. Yaiphaba and N. R. Singh, *J. Alloys Compd.*, 2014, **583**, 259.
23. L. Wang, Q. Wang, X. Xu, J. Li, L. Gao, W. Kang, J. Shi and J. Wang, *J. Mater. Chem. C*, 2013, **1**, 8033.
24. L. Wang, Z. Lv, W. Kang, X. Shangguan, J. Shi and Z. Hao, *Appl. Phys. Lett.*, 2013, **102**, 151909.
25. X. Xiao and B. Yan, *J. Alloys Compd.*, 2006, **421**, 252.
26. Z. Xu, S. Bian, J. Wang, T. Liu, L. Wang and Y. Gao, *RSC Adv.*, 2013, **3**, 1410.
27. G. Li, C. Li, Z. Xu, Z. Cheng and J. Lin, *CrystEngComm*, 2010, **12**, 4208.
28. Q. Ma, A. Zhang, M. Lu, Y. Zhou, Z. Qiu and G. Zhou, *J. Phys. Chem. B*, 2007**, 111**, 12693.
29. L. Sun, Y. Qiu, T. Liu, J. Z. Zhang, S. Dang, J. Feng, Z. Wang, H. Zhang and L. Shi, *ACS Appl. Mater. Interfaces*, 2013, **5**, 9585.
30. K. Biswas, A. D. Sontakke, R. Sen and K. Annapurna, *Spectrochim. Acta. A.*, 2013, **112**, 301.
31. J. A. Capobianco, J. C. Boyer, F. Vetrone, A. Speghini and M. Bettinelli, *Chem. Mater.*, 2002, **14**, 2915.
32. I. Földvári, A. Baraldi, R. Capelletti, N. Magnani, R. Sosa F, A. Munoz F, L. A. Kappers and A. Watterich, *Opt. Mater.*, 2007, **29**, 688.
33. N. M. Sangeetha and F. C. J. M. van Veggel, *J. Phys. Chem. C*, 2009, **113**, 14702.
34. C. Hazra, S. Sarkar and V. Mahalingam, *RSC Adv.*, 2012, **2**, 6926.
35. F. Kang and M. Peng, *Dalton Trans.*, 2014, **43**, 277.
36. G. Boulon, *J. Phys.*, (in French). 1971, **32**, 333.
37. P. Boutinaud, *Inorg. Chem.*, 2013, **52**, 6028.

RSC Advances Accepted Manuscript

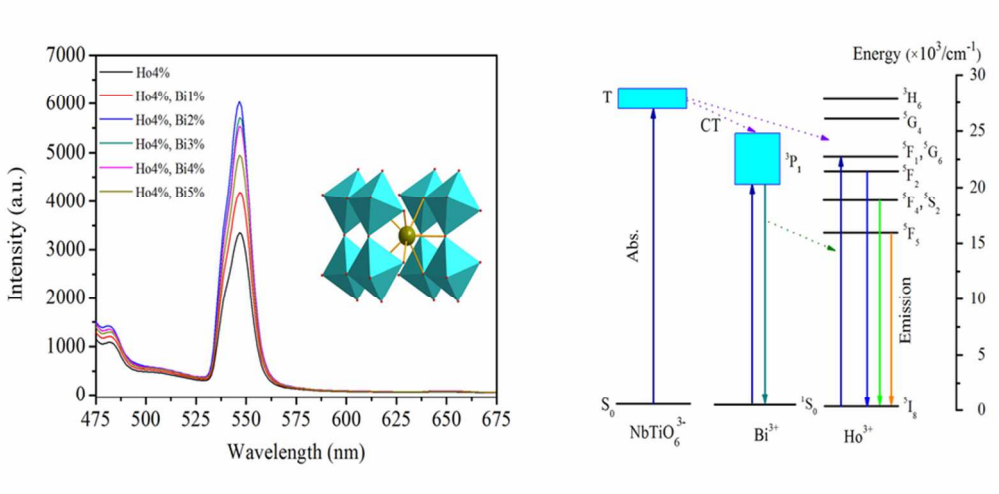

LaNbTiO6:Ho3+,Bi3+ was synthesized and the remarkably enhance of photoluminescence intensity was ascribed to efficient energy transfer from Bi3+ to Ho3+.
40x20mm (600 x 600 DPI)

RSC Advances Accepted Manuscript